ELSEVIER

Biochemical Pharmacology 61 (2001) 893–902

Biochemical Pharmacology

Metabolism of a 20-methyl substituted series of vitamin D analogs by cultured human cells: apparent reduction of 23-hydroxylation of the side chain by the 20-methyl group

V. Narayanaswamy Shankar[a], Valarie Byford[a], David E. Prosser[a], Neil J. Schroeder[b], Hugh L.J. Makin[b], Herbert Wiesinger[c], Günter Neef[c], Andreas Steinmeyer[c], Glenville Jones[a,d,*]

[a]*Department of Biochemistry, Queen's University, Kingston, ON, Canada K7L 3N6*
[b]*Department of Clinical Biochemistry, St. Bartholomew's & the Royal London School of Medicine and Dentistry, London E1 2AD, UK*
[c]*Research Laboratories of Schering AG, D-13342, Berlin, Germany*
[d]*Department of Medicine, Queen's University, Kingston, ON, Canada K7L 3N6*

Received 19 May 2000; accepted 9 August 2000

Abstract

We describe here for the first time the effect of introducing a 20-methyl group on the side-chain metabolism of the vitamin D molecule. Using a series of 20-methyl-derivatives of 1α,25-$(OH)_2D_3$ incubated with two different cultured human cell lines, HPK1A-*ras* and HepG2, previously shown to metabolize vitamin D compounds, we obtained a series of metabolic products that were identified by comparison to chemically synthesized standards on HPLC and GC-MS. 24-Hydroxylated-, 24-oxo-hydroxylated-, and 24-oxo-23-hydroxylated products of 20-methyl-1α,25-$(OH)_2D_3$ were observed, but the efficiency of 23-hydroxylation was low as compared with that of the natural hormone and, in contrast to 1α,25-$(OH)_2D_3$, no truncated 23-alcohol was formed from the 20-methyl analog. These data, taken together with results from other analogs with changes in the vicinity of the C17-C20 positions, lead us to speculate that such changes must alter the accessibility of the C-23 position to the cytochrome P450 involved. Using the HepG2 cell line, we found evidence that the 24*S*-hydroxylated product of 20-methyl-1α,25-$(OH)_2D_3$ predominates, implying that the liver cytochrome involved in metabolism is a different isoform. Studies with a more metabolically resistant analog of the series, 20-methyl-Δ^{23}-1α,25-$(OH)_2D_3$, gave the expected block in 23- and 24-hydroxylation, and evidence of an alternative pathway, namely 26-hydroxylation. 20-Methyl-Δ^{23}-1α,25-$(OH)_2D_3$ was also more potent in biological assays, and the metabolic studies reported here help us to suggest explanations for this increased potency. We conclude that the 20-methyl series of vitamin D analogs offers new perspectives into vitamin D analog action, as well as insights into the substrate preferences of the cytochrome(s) P450 involved in vitamin D catabolism.

Keywords: 20-Methyl vitamin D analogs; Cytochrome P450; Calcitriol; 1α,25-Dihydroxyvitamin D_3; Vitamin D metabolism

1. Introduction

It is now well established that the active form of vitamin D_3, 1α,25-$(OH)_2D_3$, has potent cell-differentiating/anti-proliferative activities and plays a role in calcium homeostasis [1,2]. This has led researchers to search for "non-calcemic" vitamin D analogs, those that possess anti-tumour effects without significant calcemic activity. Attention has been focused mainly upon vitamin D analogs that have modifications in the side chain. Several side-chain-modified analogs, which show favourable dissociation of effects, have already been developed for clinical use, e.g. calcipotriol [3] and 22-oxa-calcitriol [4]. The homologated series of analogs containing additional carbon atoms at the C-24 and/or C-26/C-27 positions have also been shown to possess potentially useful biological profiles [5]. We previously proposed [6] that the increased biological activity of certain members of the 20-epi series of vitamin D analogs, specif-

Abbreviations: D_2 or D_3, vitamin D_2 or vitamin D_3; OH or $(OH)_2$, hydroxy or dihydroxy; 1α,25-$(OH)_2D_3$, 1α,25-dihydroxyvitamin D_3; DPPD, *N*,*N*′-diphenylethylenediamine; FBS, fetal bovine serum; HIM, hexane/isopropanol/methanol; and MEM, Dulbecco's modified Eagle's medium.

* Corresponding author. Tel.: +613-533-2498; fax: +613-533-2987.
E-mail address: gjl@post.queensu.ca (G. Jones).

0006-2952/01/$ – see front matter
PII: S0006-2952(01)00546-9

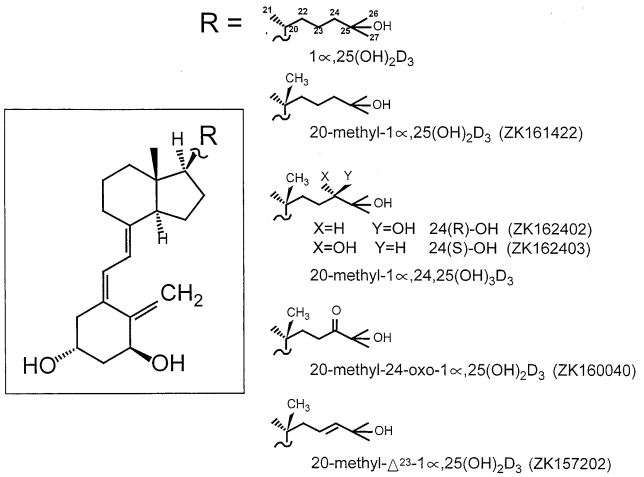

Fig. 1. Structures of 20-methyl analogs of vitamin D. Structures of the side chains of vitamin D analogs as compared with 1α,25-$(OH)_2D_3$, together with the ring structure of the vitamin D nucleus.

ically 20-epi-1α,25-$(OH)_2D_3$ (Leo Pharmaceuticals Code Name MC1288), may be partially due to altered protein binding for the vitamin D binding globulin (DBP) and the target cell vitamin D receptor (VDR) as well as a reduced rate of catabolism, particularly 23-hydroxylation, by target cell enzymes; this explanation has since been expanded [7]. It is well known that catabolism of 1α,25-$(OH)_2D_3$ in target tissues occurs through hydroxylation at either C-23 [1α,23,25-$(OH)_3D_3$] or C-24 [1α,24,25-$(OH)_3D_3$] [2]. The 23- and 24-hydroxylase activities associated with these reactions have been shown to co-localize with the same cytochrome P450, CYP24 [8].

The 20-methyl series of vitamin D analogues (Fig. 1) constitute a group of compounds with a 7- to 20-fold increase in biological activity in HL-60 cell differentiation assays compared with 1α,25-$(OH)_2D_3$, along with a wide variation in calcemic activity [9]. Since the modification in these molecules is in a region of the side chain that has been shown previously to be metabolically-sensitive to change (e.g. 20-epi-series [6,7]; 22-oxa-calcitriol [10]; 16-ene-1α,25-$(OH)_2D_3$ [11]), we hypothesized that a 20-methyl substitution might change the rate or site of metabolism by 23- and 24-hydroxylases. In the present study, metabolism of 20-methyl compounds was investigated in a human keratinocyte cell line, HPK1A-*ras*, that has been shown previously to contain high catabolic enzyme activity [12], and in a human hepatoma cell line, HepG2, previously shown to be capable of side-chain modifications of a number of vitamin D analogs [10,13]. In this study we set out:

(a) To compare qualitatively and quantitatively the *in vitro* metabolism of 20-methyl-1α,25-$(OH)_2D_3$ and 1α,25-$(OH)_2D_3$ in the HPK1A-*ras* keratinocyte, a well characterized vitamin D target cell.
(b) To examine the metabolism of other 20-methyl analogs including 20-methyl-Δ^{23}-1α,25-$(OH)_2D_3$ in the same keratinocyte model.
(c) To examine cell-specific differences in the metabolism of 20-methyl-1α,25-$(OH)_2D_3$ by comparing metabolism in the HepG2 hepatoma and the HPK1A-*ras* keratinocyte cell line.

2. Materials and methods

2.1. Materials

1α,25-$(OH)_2D_3$ was a gift from Dr. M. Uskokovic (Hoffmann-LaRoche). The test vitamin D analogs (see Fig. 1): ZK-161422, 20-methyl-1α,25-$(OH)_2D_3$; ZK-157202, 20-methyl-Δ^{23}-1α,25-$(OH)_2D_3$; ZK-160040, 20-methyl-24-oxo-1α,25-$(OH)_2D_3$; ZK-162402, 20-methyl-1α,24*R*,25-$(OH)_3D_3$; and ZK-162403, 20-methyl-1α,24*S*,25-$(OH)_3D_3$ were synthesized by Schering AG, [9]. [1β-^{3}H]1α,25-$(OH)_2D_3$ (3 Ci/mmol) was prepared earlier in our laboratory [14]. The human keratinocyte cell line [15] transfected with the *ras* proto-oncogene [16], HPK1A-*ras*, was the gift of Dr. R. Kremer (Royal Victoria Hospital, McGill University). HepG2 cells were obtained from the American Type Culture Collection. All solvents used were of HPLC grade and were obtained from Caledon. Trypsin, penicillin G, gentamycin, fungizone, and MEM were purchased from GIBCO. FBS was from ICN. DPPD was purchased from the Sigma Chemical Co., and BSA was obtained from Boehringer Mannheim.

2.2. Cell culture and incubation with vitamin D analogs

HPK1A-*ras* cells were grown to confluence in MEM supplemented with penicillin G (100 μg/mL), gentamycin (5 μg/mL), and fungizone (300 ng/mL) containing 10% FBS as previously described [10,12]. Near confluence, 1α,25-$(OH)_2D_3$ (10 nM) was added to the culture medium to induce the catabolic enzymes. Medium was removed 24 hr later, and cells were then incubated with 1α,25-$(OH)_2D_3$ or 20-methyl analogs (to achieve a final concentration of 10 μM added in 0.01% EtOH) for 48 hr in Dulbecco's culture medium (10 mL/plate) supplemented with 100 μM DPPD and 1% BSA. No-cell controls consisted of 10 mL of the medium and the analog (10 μM in 0.01% EtOH) incubated in the absence of cells for the same length of time. In time-course experiments, cells were subcultured into 6-well plates and incubated with a 10 μM concentration of a vitamin D analog in FBS-free medium supplemented with DPPD and 1% BSA for 0, 4, 8, 24, or 48 hr.

Hep-G2 cells were grown in MEM containing 5% FBS and antibiotics (100 μg/mL of penicillin G, 5 μg/mL of gentamycin, and 300 ng/mL of fungizone) as previously described [10]. Cells were then incubated for 48 hr with a vitamin D analog (10 μM in 0.01% EtOH) in MEM (10 mL/plate) supplemented with 100 μM DPPD and 1% BSA. No-cell controls consisted of 10 mL of medium and a

vitamin D analog (10 μM in 0.01% EtOH) incubated for the same length of time.

2.3. Lipid extraction and purification of metabolites

Cells and medium were extracted using a modification of the method of Bligh and Dyer [17], in which chloroform was replaced by methylene chloride. After addition of methanol, which constitutes the first step of extraction, approximately 2 μg of 1α-OH-D_3 was added to each incubation in order to assess losses during extraction and HPLC steps. Recoveries of this internal standard routinely averaged in the 85–90% range. During extraction, the organic layer was evaporated to dryness under a stream of nitrogen, redissolved in hexane/isopropanol/methanol (91:7:2, by vol., HIM) and subjected to purification by HPLC.

A semi-preparative scale HPLC of metabolites of 20-methyl-analogs was performed on a modular system consisting of a model 590 pump, a U6K manual injector, a model 440 fixed wavelength detector (254 nm), and/or a model 990 photodiode array detector (Waters Scientific). 20-Methyl analogs possess the typical λ_{max} = 265 nm ($\varepsilon \sim$ 17,500) expected for all vitamin D compounds possessing the *cis*-triene system. Hence, HPLC chromatograms were monitored at 265 nm and for the classical vitamin D chromophore (λ_{max} = 265 nm; λ_{min} = 228 nm). Separation of metabolites in lipid extracts was achieved initially using a 3 μm Zorbax-SIL (0.62 × 8 cm) column eluted with HIM (91:7:2) at a flow rate of 1 mL/min. Peaks showing the classical vitamin D chromophore were collected and repurified using a Zorbax-CN (0.46 × 25 cm) column with HIM 91:7:2 at a flow rate of 1 mL/min. Metabolites were considered sufficiently pure for mass spectral and chemical analyses when they gave a single peak on HPLC.

Analytical scale HPLC was performed on time-course samples using an Alliance system (Waters Scientific) fitted with the same column and eluted with the same solvent system as described above [18].

2.4. Derivatization and GC-MS

Per-trimethylsilyl ethers of the metabolites were prepared using the reagent *N*-trimethylsilylimidazole, and the derivatives were subjected to GC-MS using a Hewlett-Packard 5970 mass selective detector in positive ion electron impact mode, as previously described [19,20]. Electron impact spectra were recorded across each peak and stored. Mass spectra used for final identification purposes were obtained by averaging the spectra from each peak and subtracting the background.

2.5. Vitamin D side-chain modelling

Side-chain conformations were adapted from the crystal structure for ergocalciferol (ergcal10) retrieved from the Cambridge Crystallographic Database and the structure for calciferol in the SYBYL v6.6 (Tripos Associates) library. Chiral carbons were inverted (e.g. 20-epi), atom types were added (e.g. 25-hydroxyl or 20-methyl), or atom types were modified (sp2 carbons in 16-ene) by using SYBYL running on a Silicon Graphics Inc. octane system. Structures with hydrogens were minimized to convergence [0.05 kcal/(mol · Å)] using the Powell conjugate gradient termination method with the Tripos forcefield, Gasteiger-Marsili charges, and a distance-dependent dielectric. Figures were produced using Weblab (Molecular Simulations Inc.).

3. Results

3.1. Comparison of the metabolism of 20-methyl-1α,25-$(OH)_2D_3$ and 1α,25-$(OH)_2D_3$ by HPK1A-ras cells

Incubation of HPK1A-*ras* cells with 20-methyl-1α,25-$(OH)_2D_3$ resulted in the formation of two identifiable metabolites (Table 1 and Fig. 2A), both of which possessed the chromophore of vitamin D. These metabolites were not formed when 20-methyl-1α,25-$(OH)_2D_3$ was incubated with medium in the absence of cells or when cells were incubated with medium alone (data not shown). Fig. 2B shows the results of an incubation with 1α,25-$(OH)_2D_3$ with the same cells under identical conditions. Characterization of the metabolites of 1α,25-$(OH)_2D_3$ in this system has been described previously [12], and thus in Fig. 2B each metabolite is labelled appropriately. Characterization of metabolites of 20-methyl-1α,25-$(OH)_2D_3$ is discussed below.

3.2. Characterization of metabolites of 20-methyl-1α,25-$(OH)_2D_3$ from HPK1A-ras cells

3.2.1. Metabolite 1: 20-methyl-24-oxo-1α,25-$(OH)_2D_3$

Although insufficient material was available for GC-MS, co-migrational analysis on Zorbax-SIL with a standard compound was possible (Table 2). These data together with other retention data from Zorbax-CN revealed that Metabolite 1 co-migrates with and can be tentatively identified as 20-methyl-24-oxo-1α,25-$(OH)_2D_3$.

3.2.2. Metabolite 2: 20-methyl-1α,24R,25-$(OH)_3D_3$

Metabolite 2 co-migrated with 20-methyl-1α,24*R*,25-$(OH)_3D_3$ on two HPLC systems and had the same relative retention time on GC (Table 1). The mass spectrum of the per-trimethylsilylated derivative of Metabolite 2 (Fig. 3A) featured a molecular ion of *m/z* 734, indicating a hydroxylated version of 20-methyl-1α,25-$(OH)_2D_3$. The major fragment that can be observed in the spectrum at *m/z* 131 is probably derived from cleavage of the C24-C25 bond, implying an unchanged C25-C27 moiety. Moreover, the fragility of this C24-C25 bond suggests that the additional hydroxyl group is probably at C-24. Other major fragments present in the mass spectrum included: *m/z* 644 $(M\text{-}90)^+$, 603 $(M\text{-}131)^+$, 554 $(M\text{-}90\text{-}90)^+$, 513 $(M\text{-}131\text{-}90)^+$, and 423

Table 1
Characterization of metabolites of 24-substituted 20-methyl-1α,25-$(OH)_2D_3$ analogs generated in HPK1A-*ras* cells

Starting compound / Product	HPLC analysis Retention time (min)		GC relative retention Time[d] (min)	Mass spectral analysis[e] (*m/z*)		Putative identity
	Z-SIL[a,b]	Z-CN[c]		Molecular ion	Other major ions	
20-CH_3-1α,25-$(OH)_2D_3$[f]	14.00[a]	11.50	1.296	646	631,515,466,425,299,224,131	20-CH_3-1α,25-$(OH)_2D_3$
20-CH_3-1α,25-$(OH)_2D_3$ Met 1	18.10[a]	15.82	ND	ND	ND	20-CH_3-24-oxo-1α,25-$(OH)_2D_3$ (see Table 2)
20-CH_3-1α,25-$(OH)_2D_3$ Met 2	26.50[a]	17.71	1.536	734	644,603,513,423,341,251,217,131	20-CH_3-1α,24*R*,25-$(OH)_3D_3$
20-CH_3-1α,24*R*,25-$(OH)_3D_3$[f]	17.74[b]	17.04	1.533	734	644,603,513,423,341,251,217,131	20-CH_3-1α,24*R*,25-$(OH)_3D_3$
20-CH_3-1α,24*R*,25-$(OH)_3D_3$ Met 1	12.67[b]	15.60	1.467	660	570,529,480,341,251,217,131	20-CH_3-24-oxo-1α,25-$(OH)_2D_3$
20-CH_3-1α,24*R*,25-$(OH)_3D_3$ Met 2	15.86[b]	16.80	1.742	734	644,603,513,423,341,251,217,131	?3-epi-20-CH_3-1α,24*R*,25-$(OH)_3D_3$?
20-CH_3-1α,24*R*,25-$(OH)_3D_3$ Met 3	15.86[b]	20.02	1.737	748	658,617,499,473,409,383,293,217,131	20-CH_3-24-oxo-1α,23,25-$(OH)_3D_3$
20-CH_3-1α,24*R*,25-$(OH)_3D_3$ Met 4	21.02[b]	26.70	ND	ND	ND	Unknown
20-CH_3-1α,24*S*,25-$(OH)_3D_3$[f]	16.61[b]	17.11	1.541	734	644,603,513,423,341,251,217,131	20-CH_3-1α,24*S*,25-$(OH)_3D_3$
20-CH_3-1α,24*S*,25-$(OH)_3D_3$ Met 1	12.66[b]	15.76	ND	ND	ND	20-CH_3-24-oxo-1α,25-$(OH)_2D_3$
20-CH_3-1α,24*S*,25-$(OH)_3D_3$ Met 4	21.20[b]	23.3	ND	ND	ND	Unknown
20-CH_3-1α,24*S*,25-$(OH)_3D_3$ Met 5A[g]	21.20[b]	26.89	1.666	748	613,525,435,345,275,185	Unknown
20-CH_3-1α,24*S*,25-$(OH)_3D_3$ Met 5B[g]	21.20[b]	26.89	1.799	748	658,617,473,371,299,219	20-CH_3-24-oxo-1α,25,26-$(OH)_3D_3$
20-CH_3-24-oxo-1α,25-$(OH)_2D_3$[f]	11.78[b]	15.79	1.478	660	570,529,480,341,251,217,131	20-CH_3-24-oxo-1α,25-$(OH)_2D_3$
20-CH_3-24-oxo-1α,25-$(OH)_2D_3$ Met 1	14.83[b]	20.21	1.734	748	658,617,499,473,409,383,293,217,131	20-CH_3-24-oxo-1α,23,25-$(OH)_3D_3$
20-CH_3-24-oxo-1α,25-$(OH)_2D_3$ Met 2	20.48[b]	27.20	1.534	734	644,603,513,423,341,251,217,131	20-CH_3-1α,24*R*,25-$(OH)_3D_3$

[a] HPLC conditions: Zorbax-SIL (3 μm, 0.62 $\times$ 8 cm) column, 91/7/2 HIM (1.0 mL/min) solvent system.
[b] HPLC conditions: Zorbax-SIL (3 μm, 0.62 $\times$ 8 cm) column, 91/7/2 HIM (1.5 mL/min) solvent system.
[c] HPLC conditions: Zorbax-CN (6 μm, 0.46 $\times$ 25 cm) column, 91/7/2 HIM (1.0 mL/min) solvent system.
[d] GC conditions: HP-1 cross-linked methyl silicone gum column with helium as the carrier gas at a flow rate of 1 mL/min. Dihydrotachysterol (DHT_3) was used as an external standard.
[e] Ions from mass spectrum used to identify metabolites.
[f] Chemically synthesized material.
[g] Metabolite 5 splits into two peaks on GC.
ND = not determined.

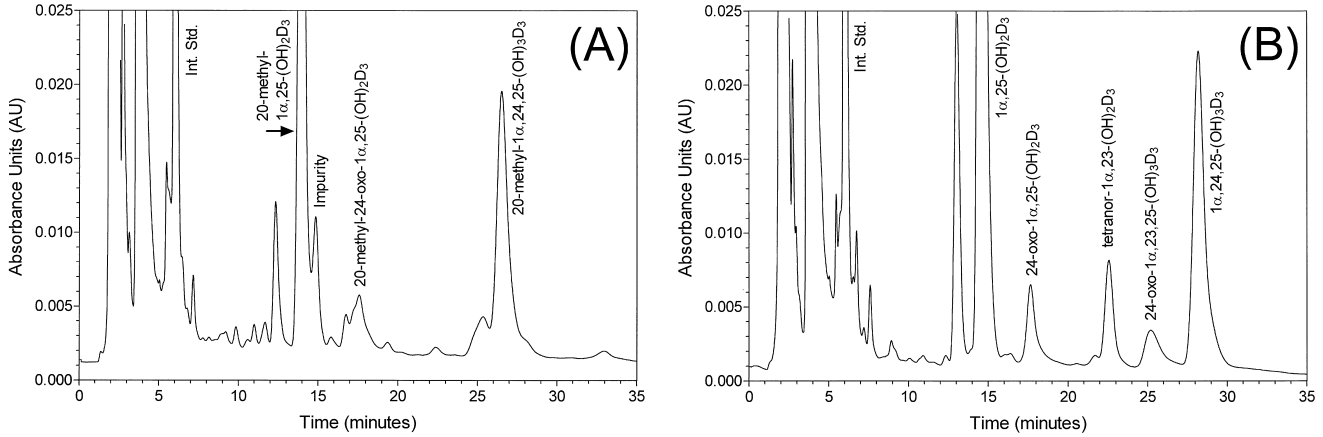

Fig. 2. HPLC profile of the lipid extract from HPK1A-*ras* cells incubated with: (A) 20-methyl-1α,25-$(OH)_2D_3$ and (B) 1α,25-$(OH)_2D_3$ for 48 hr. Total lipid extracts were separated on a Zorbax-SIL column using the solvent HIM (91:7:2) at a flow rate of 1 mL/min. Metabolites of 20-methyl-1α,25-$(OH)_2D_3$ were identified based upon the presence of the classical vitamin D chromophore (λ_{max} = 265 nm; λ_{min} = 228 nm). Metabolites of 1α,25-$(OH)_2D_3$ were identified based upon comparison of retention times to known authentic standards. These traces, which represent the 48-hr time point, are abstracted from time-course studies described in the text and analysed in Fig. 4. The peak at 6 min, marked Int Std, is the internal standard, 1α-OH-D_3, added for assessing extraction losses.

$(M\text{-}131\text{-}90\text{-}90)^+$, which are the result of sequential losses of TMSiOH from the molecular ion or its major *m/z* 603 fragment, which results from A-ring cleavage. Additional fragments at *m/z* 341 and 251 resulted from sequential losses of TMSiOH from the molecular ion, which had lost the complete side chain (431 a.m.u.) through C17-C20 cleavage. These fragments also confirm a side-chain location for the extra hydroxyl function. The expected fragment at *m/z* 217 arose from cleavage in the A ring and confirms retention of the 1α-hydroxylated nucleus. This fragmentation is found in the TMS-derivatized spectra of most 1α-hydroxylated vitamin D compounds [21]. The mass spectrum of synthetic 20-methyl-1α,24*R*,25-$(OH)_3D_3$ was found to be virtually identical to that of Metabolite 2 (Fig. 3B). We conclude that Metabolite 2 is 20-methyl-1α,24*R*,25-$(OH)_3D_3$.

Table 2
Co-chromatography of the putative 24-oxo metabolite generated from 20-methyl-1α,25-$(OH)_2D_3$ and 24-substituted 20-methyl-1α,25-$(OH)_2D_3$ analogs with the synthetic standard

Source of 24-oxo-compound	Relative retention time[a]
20-CH_3-24-oxo-1α,25$(OH)_2D_3$[b]	2.907 ± 0.001
20-CH_3-1α,24*R*,25-$(OH)_3D_3$ Met 1	2.900 ± 0.008
20-CH_3,1α,24*S*,25-$(OH)_3D_3$ Met 1	2.891 ± 0.016
20-CH_3-1α,25-$(OH)_2D_3$ Met 1	2.892 ± 0.015

[a] HPLC conditions: Zorbax-SIL (3 μm, 0.62 × 8 cm) column, 91/7/2 HIM (1.0 mL/min) solvent system. 25-OH-D_3 was used as the internal standard.

[b] Synthetic standard: ZK 160040.

Values are means ± SEM, N = 3.

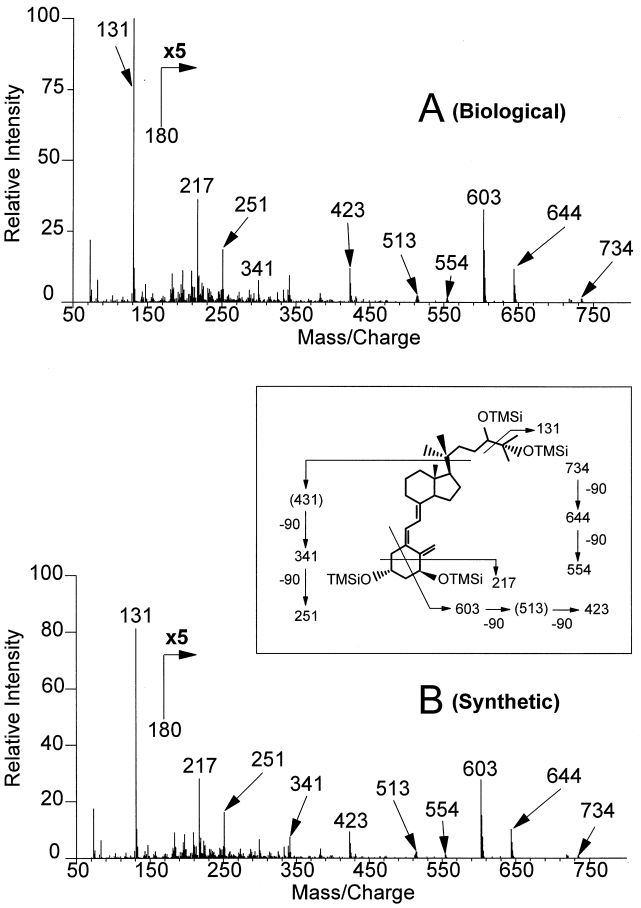

Fig. 3. Mass spectra of (A) the putative monohydroxylated metabolite (Metabolite 2) from 20-methyl-1α,25-$(OH)_2D_3$ and (B) chemically synthesized 20-methyl-1α,24*R*,25-$(OH)_3D_3$. TMSi derivatives of the purified metabolite (Metabolite 1) and its corresponding synthetic standard were subjected to GC-MS on an HP-1 cross-linked methyl silicone gum column with helium as a carrier gas at a flow rate of 1 mL/min. Mass spectra shown are those of the pyro-isomer and were obtained by averaging each peak and subtracting the background. The fragmentation patterns depicted are those of the actual TMSi derivatives prior to cyclization.

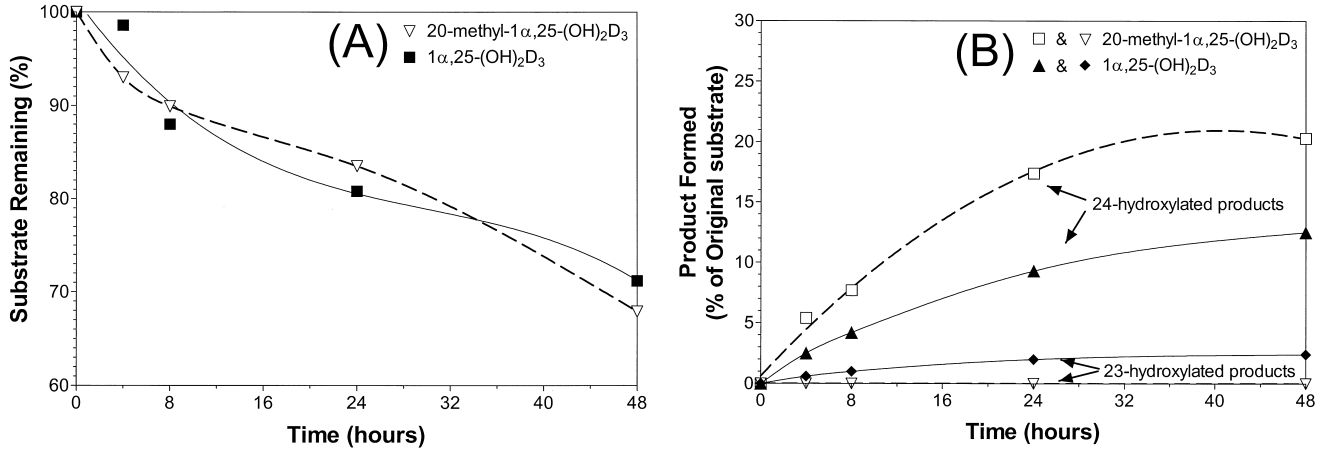

Fig. 4. (A) Rate of disappearance of substrate and (B) rate of formation of 24-hydroxylated and 23-truncated metabolites of 20-methyl-1α,25-$(OH)_2D_3$ and 1α,25-$(OH)_2D_3$ in HPK1A-*ras* cells. The time-course studies, from which Fig. 2 was derived, were performed in duplicate wells of a 6-well plate before each incubation was extracted and analysed on HPLC. To compensate for losses during analysis, approximately 2 μg 1α-OH-D_3 was added to each well during the extraction process. Recoveries were routinely around 85–90%. HPLC peaks were integrated, and remaining substrate and recovered products (24- or 23-hydroxylated metabolites) were then expressed as a percentage of the substrate present at 0 hr. Data in the experiment depicted represent reproducible trends observed in three separate time-course studies.

*3.3. Quantitative aspects of the metabolism of 20-methyl-1α,25-$(OH)_2D_3$ and 1α,25-$(OH)_2D_3$ by HPK1A-*ras *cells*

Time-course studies of the disappearance of substrate and the rate of formation of 24-hydroxylated metabolites from both of these substrates are illustrated in Fig. 4, together with the formation of the 24,25,26,27-tetranor-1α,23-$(OH)_2D_3$ from 1α,25-$(OH)_2D_3$. No equivalent metabolite from 20-methyl-24-oxo-1α,25-$(OH)_2D_3$ could be observed. This graph clearly shows that despite enhanced 24-hydroxylation of the 20-methyl substrate, C23-C24 cleavage to give a tetranor-23-alcohol did not appear to occur. Substrate disappearance for both compounds was similar. By 48 hr of incubation, there was a small loss (10–15%) of recovered material (substrate remaining + products formed), which was similar for both substrates.

*3.4. Further metabolism of 24-substituted 20-methyl-1α,25-$(OH)_2D_3$ analogs in HPK1A-*ras *cells*

Other metabolites of 20-methyl-1α,25-$(OH)_2D_3$ along the C-24 oxidation pathway including 20-methyl-1α,24*R*,25-$(OH)_3D_3$, 20-methyl-1α,24*S*,25-$(OH)_3D_3$, and 20-methyl-24-oxo-1α,25-$(OH)_2D_3$ were synthesized and incubated with HPK1A-*ras* cells. Our results are summarized in Table 1. Products were again identified by a combination of HPLC retention times and GC-MS. It can be seen that, as expected, the main product of 20-methyl-1α,25-$(OH)_2D_3$ metabolism, 20-methyl-1α,24*R*,25-$(OH)_3D_3$, was further metabolized to 20-methyl-24-oxo-1α,25-$(OH)_2D_3$ and 20-methyl-24-oxo-1α,23,25-$(OH)_3D_3$, although the amount of this latter 23-hydroxylated compound was less than that obtained from the 23-hydroxylation of the natural hormone, 1α,25-$(OH)_2D_3$, and formation of the tetranor-23-alcohol was still not observed. Interestingly, the synthetic 24*S*-isomer, although not formed in HPK1A-*ras* cells *in vitro*, can also be converted to the 24-oxo derivative (see also Table 2).

*3.5. Metabolism of 20-methyl-Δ^{23}-1α,25-$(OH)_2D_3$ by HPK1A-*ras *cells*

We studied the metabolism of this analog in order to assess the effect of the introduction of the C23-C24 double bond on the 24- and 23-hydroxylase activities of HPK1A-*ras* cells. As expected, the metabolic stability of this analog was changed by this side-chain modification (Fig. 5A). Even after 48 hr of incubation, >95% of the recovered material was the unchanged unsaturated substrate compared with the 75% observed for 20-methyl-1α,25-$(OH)_2D_3$. In addition, only one hydroxylated product (Metabolite 1) could be discerned in the HPLC profile, and this metabolite was putatively identified by GC-MS as 20-methyl-Δ^{23}-1α,25,26-$(OH)_3D_3$ (Fig. 5B). Although the identification is not definitive, the mass spectrum features a molecular ion of *m/z* 732, indicating hydroxylation and retention of the C23-C24 double bond, together with a fragment at *m/z* 103, which has been observed in the spectra of a number of other 26(27)-hydroxylated vitamin D analogs previously [21–23]. Other major fragments included: *m/z* 642 $(M\text{-}90)^+$, 629 $(M\text{-}103)^+$, 601 $(M\text{-}131)^+$, 552 $(M\text{-}90\text{-}90)^+$, 539 $(M\text{-}90\text{-}103)^+$, 473 (C20-C22 bond cleavage), 383 (473-90), and 293 (473-90-90). These latter three fragments are caused by the presence of the C23-C24 double bond and/or the C-20 methyl group and pinpoint the additional hydroxyl group to a site distal to C-24. We conclude that Metabolite 1 is probably 20-methyl-Δ^{23}-1α,25,26-$(OH)_3D_3$.

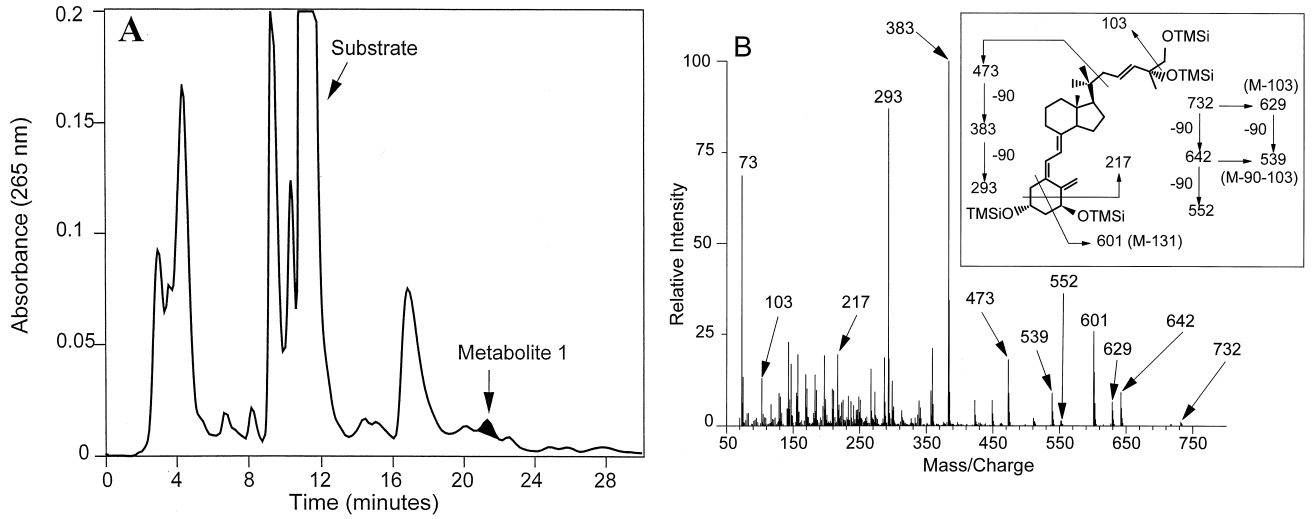

Fig. 5. (A) HPLC profile of the lipid extract from HPK1A-*ras* cells incubated with 20-methyl-Δ^{23}-1α,25-$(OH)_2D_3$. Total lipid extract was separated on a Zorbax-SIL column using the solvent HIM (91:7:2) at a flow rate of 1 mL/min. The metabolite of 20-methyl-Δ^{23}-1α,25-$(OH)_2D_3$ was identified based upon the presence of the classical vitamin D chromophore (λ_{max} = 265 nm; λ_{min} = 228 nm) and has been shaded. (B) Mass spectrum of metabolite from 20-methyl-Δ^{23}-1α,25-$(OH)_2D_3$. The TMSi derivative of the purified metabolite was subjected to GC-MS on an HP-1 cross-linked methyl silicone gum column with helium as a carrier gas at a flow rate of 1 mL/min. The mass spectrum shown is that of the pyro-isomer and was obtained by averaging each peak and subtracting the background. The fragmentation patterns depicted are those of the actual TMSi derivative prior to cyclization.

3.6. Metabolism of 20-methyl-1α,25-$(OH)_2D_3$ by Hep-G2 cells

Metabolism of 20-methyl-1α,25-$(OH)_2D_3$ in HepG2 cells resulted in the formation of six metabolites (Fig. 6) that possessed the same UV chromophore as the substrate, only two of which were identified (Table 3). The main metabolite (Metabolite 1) co-migrated with 20-methyl-1α,24*S*,25-$(OH)_3D_3$ on HPLC and GC and possessed a mass spectrum consistent with this identity; the more polar Metabolite 2 had a mass spectrum consistent with a structure containing a 26-hydroxyl group. This metabolite was not observed in HPK1A-*ras* cells.

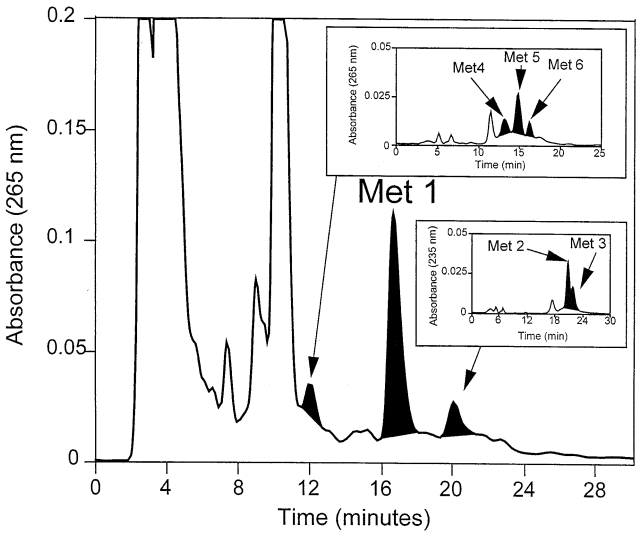

Fig. 6. HPLC profile of the lipid extract from Hep-G2 cells incubated with 20-methyl-1α,25-$(OH)_2D_3$. Total lipid extract was separated on a Zorbax-SIL column using the solvent HIM (91:7:2) at a flow rate of 1 mL/min. Metabolites of 20-methyl-1α,25-$(OH)_2D_3$ were identified based upon the presence of the classical vitamin D chromophore (λ_{max} = 265 nm; λ_{min} = 228 nm) and have been shaded.

Incubation of Hep-G2 cells with the 24-oxo and 24-hydroxylated compounds of the 20-methyl series gave rise to any one of the combination of 24-oxidized products (Table 3) but gave no evidence of the 23-hydroxylated products that was produced in HPK1A-*ras* cells. Unlike the pattern found in the HPK1A-*ras* cell line, the pattern found in the HepG2 cell line favours a 24-*S* stereochemistry for the 24-hydroxylation reaction using 20-methyl-1α,25-$(OH)_2D_3$ or 20-methyl-24-oxo-1α,25-$(OH)_2D_3$ as the substrate.

4. Discussion

In this paper, we have demonstrated that 20-methyl-1α,25-$(OH)_2D_3$ is metabolized *in vitro* by two different cultured human cell lines to side-chain-hydroxylated metabolites identified as 24-oxidized products analogous to compounds formed in the C-24 oxidation pathway from the hormone 1α,25-$(OH)_2D_3$ [14]. Their identification rested on two different approaches, one involving direct interpretation of mass spectral evidence acquired from GC-MS and the other from co-chromatography of the metabolites with chemically synthesized authentic standards. Incubation of chemically synthesized versions of metabolic products of 20-methyl-1α,25-$(OH)_2D_3$ with cultured cells reinforced our view that the later metabolic products are 24- and 23-hydroxylated, indicating the existence of a pathway similar to that found for the natural hormone. Work with 20-

Table 3
Characterization of metabolites of 20-methyl-1α,25-$(OH)_2D_3$ and its 24-substituted analogs generated in Hep G2 cells

Starting compound / Product	HPLC analysis Retention time (min)		GC relative retention time[c] (min)	Mass spectral analysis[d] (*m/z*)		Putative identity
	Z-SIL[a]	Z-CN[b]		Molecular ion	Other major ions	
20-CH_3-1α,25-$(OH)_2D_3$[e]	10.06	11.44	1.296	646	631,515,466,425,299,224,131	20-CH_3-1α,25-$(OH)_2D_3$
20-CH_3-1α,25-$(OH)_2D_3$ Met 1	16.59	17.77	1.541	734	644,603,423,341,251,217,131	20-CH_3-1α,24*S*,25-$(OH)_3D_3$
20-CH_3-1α,25-$(OH)_2D_3$ Met 2	19.97	20.78	1.582	734	719,631,541,451,399,251,219	20-CH_3-1α,25,26-$(OH)_3D_3$
20-CH_3-1α,24*R*,25-$(OH)_3D_3$[e]	21.33	18.44	1.533	734	644,603,423,341,251,217,131	20-CH_3-1α,24*R*,25-$(OH)_3D_3$
20-CH_3-1α,24*R*,25-$(OH)_3D_3$ Met 1	14.39	16.47	1.471	660	570,529,480,341,251,217,131	20-CH_3-24-oxo-1α,25-$(OH)_2D_3$
20-CH_3-1α,24*R*,25-$(OH)_3D_3$ Met 2	18.69	17.91	1.743	734	644,603,423,341,251,217,131	?3-epi-20-CH_3-1α,24*R*,25-$(OH)_3D_3$?
20-CH_3-1α,24*S*,25-$(OH)_3D_3$[e]	20.37	19.89	1.535	734	644,603,423,341,251,217,131	20-CH_3-1α,24*S*,25-$(OH)_3D_3$
20-CH_3-1α,24*S*,25-$(OH)_3D_3$ Met 1	12.86	18.00	1.471	660	570,529,480,341,251,217,131	20-CH_3-24-oxo-1α,25-$(OH)_2D_3$
20-CH_3-1α,24*S*,25-$(OH)_3D_3$ Met 2	17.46	18.68	1.514	734	644,603,423,341,251,217,131	?3-epi-20-CH_3-1α,24*S*,25-$(OH)_3D_3$?
20-CH_3-24-oxo-1α,25-$(OH)_2D_3$[e]	11.57	16.47	1.465	660	570,529,480,341,251,217,131	20-CH_3-24-oxo-1α,25-$(OH)_2D_3$
20-CH_3-24-oxo-1α,25-$(OH)_2D_3$ Met 1	16.22	18.12	1.542	734	644,603,423,341,251,217,131	20-CH_3-1α,24*S*,25-$(OH)_3D_3$
20-CH_3-24-oxo-1α,25-$(OH)_2D_3$ Met 2	21.08	24.46	1.793	748	658,617,503,399,326,219	20-CH_3-24-oxo-1α,25,26-$(OH)_3D_3$

[a] HPLC conditions: Zorbax-SIL (3 μm, 0.62 × 8 cm) column, 91/7/2 HIM (1.0 mL/min) solvent system.
[b] HPLC conditions: Zorbax-CN (6 μm, 0.46 × 25 cm) column, 91/7/2 HIM (1.0 mL/min) solvent system.
[c] GC conditions: HP-1 cross-linked methyl silicone gum column with helium as the carrier gas at a flow rate of 1 mL/min; relative retention time with respect to dihydrotachysterol (DHT_3).
[d] Ions from mass spectrum used to identify metabolites.
[e] Chemically synthesized material.

methyl-Δ^{23}-1α,25-$(OH)_2D_3$, a compound that is metabolized at a reduced rate as compared with 20-methyl-1α,25-$(OH)_2D_3$ and 1α,25-$(OH)_2D_3$, further emphasizes the importance of C-24 oxidation to this metabolic inactivation process. As with other metabolically resistant molecules studied to date, the blockade of the C-23 and C-24 positions appears to shift the site of hydroxylation to the terminus of the molecule, albeit at lower efficiency [21,22].

The finding that the amount of 23-hydroxylated metabolites of 20-methyl-1α,25-$(OH)_2D_3$ is low in these studies implies that the 23-hydroxylation reaction might be adversely affected by 20-methyl substitution. In fact, 23-hydroxylation is similarly sensitive to the introduction of a C16-C17 double bond into the D-ring of 16-ene-1α,25-$(OH)_2D_3$ [11] and the inversion of the stereochemistry at C-20 in 20-epi-1α,25-$(OH)_2D_3$ [6,7]. The evidence suggests that 23-hydroxylation is carried out by CYP24, the cytochrome P450 also thought to be responsible for 24-hydroxylation [2]. In addition, it is thought that intermediates of the C-24 oxidation pathway are only displaced from the enzyme when high concentrations of 1α,25-$(OH)_2D_3$ or its analogs are used, as was the case in the experiments performed here. Thus, it is our view that modifications around the C17-C20 bond must subtly change the binding of substrate and enzyme, which in turn profoundly influences the rate of 23-hydroxylation and subsequent side-chain cleavage to the water-soluble calcitroic acid but not the rate of 24-hydroxylation. Alternatively, modifications around the C17-C20 bond may also alter the ability of the substrate to displace the 23-hydroxylated intermediate from the active site of CYP24. Molecular modelling (Fig. 7) shows the radically different orientation of the side-chain of 20-methyl and 20-epi analogs as compared with the natural hormone, 1α,25-$(OH)_2D_3$ [24]. Equally striking is the similarity of the conformation assumed by the two 20-modified analogs (Fig. 7 and Ref. 24). However, it is not immediately clear why this conformation of the side chain in 20-methyl-1α,25-$(OH)_2D_3$ and 20-epi-1α,25-$(OH)_2D_3$ leads to changes in the hydroxylation rate at C-23 but not C-24.

These studies confirm previous data [12] which suggested that hepatoma cells are capable of the 24*S*-hydroxylation of the unsubstituted side chain of vitamin D compounds, as well as the further oxidation of an existing 24-hydroxyl function to the 24-ketone. In contrast, the conventional target-cell 24-hydroxylase, CYP24, introduces a 24-hydroxyl group stereo-specifically in the 24*R*-configuration [25]. Furthermore, liver cell 24-hydroxylation is never accompanied by 23-hydroxylation even for 1α,25-$(OH)_2D_3$, whereas target-cell metabolism often includes 23-hydroxylation, even though on occasion the efficiency of this process can be reduced. Therefore, this work implies that 20-methyl-1α,25-$(OH)_2D_3$ is a substrate for at least two different cytochromes P450 in liver and target cells.

The finding that the 24-hydroxylated metabolites of 20-methyl-1α,25-$(OH)_2D_3$ predominate in both liver and target cells poses the question as to whether these metabolites

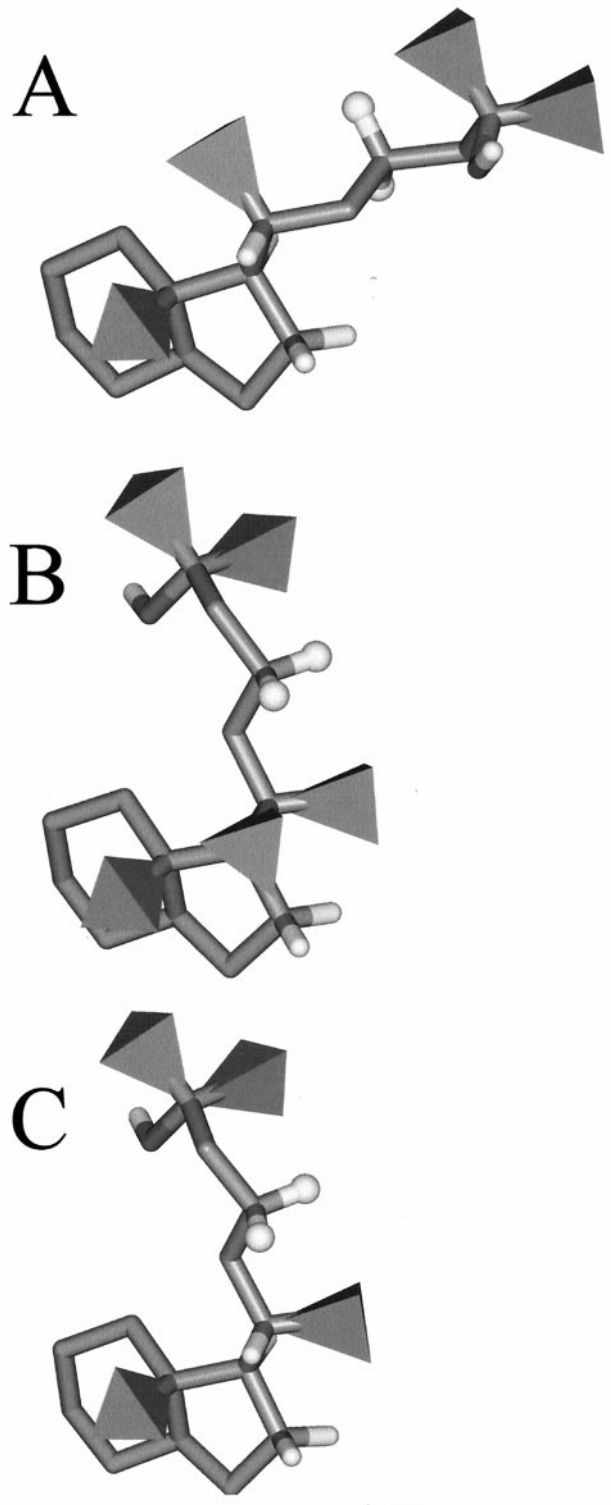

Fig. 7. Models showing how modifications around the C17-C20 change the side-chain conformation. Side-chain orientations of (A) vitamin D_3 (top), (B) 20-methyl vitamin D_3 (middle), and (C) 20-epi vitamin D_3 (bottom) relative to the C- and D-rings. Methyl groups are depicted as tetrahedra and the hydrogen atoms at C23 as spheres. The native side-chain of vitamin D_3 is shown in the preferred gauche (+) orientation about the C16-C17-C18-C19 torsion angle as described previously [24]. The analog modifications at C20 conformationally restrict the side-chain to the anti-orientation about the C16-C17-C18-C19 angle, which is lower in energy than either gauche (+) or (−) orientation.

contribute to the biological activity previously ascribed to the parent compound [9,26]. Assays performed on the chemically synthesized 24-hydroxylated metabolites (ZK-162402 and ZK-162403) suggest that the cell-differentiating activity of 20-methyl-1α,25-$(OH)_2D_3$ is retained in these two metabolites but that there is a significant (~100-fold) reduction of calcemic activity [9]. This may be due to the relative stability of 24-hydroxylated metabolites of 20-methyl-1α,25-$(OH)_2D_3$ in target cell systems, whereas *in vivo* other factors, such as hepatic clearance and poor DBP binding, play a significant role and limit survival of the metabolites.

The Δ^{23}-derivative of 20-methyl-1α,25-$(OH)_2D_3$ (ZK-157202) was also found to be relatively resistant to metabolism in our *in vitro* liver and target cell systems. In contrast, these results are easier to rationalize given the higher biological activity observed for Δ^{23}-20-methyl-1α,25-$(OH)_2D_3$ as compared with 20-methyl-1α,25-$(OH)_2D_3$ or 1α,25-$(OH)_2D_3$ in *both* cell differentiation and calcemic assays [9,26]. One could argue that our finding that Δ^{23}-20-methyl-1α,25-$(OH)_2D_3$ was not metabolized by the C-24 oxidation pathway allows it to be retained longer inside all target cells, those involved in calcemic as well as cell differentiation responses. Of course, other important parameters such as VDR- and DBP-binding of this compound would also need to be considered before making a broad-based conclusion of this type [2,27].

Acknowledgments

This work was supported by grants from the Medical Research Council of Canada. We acknowledge the important contribution of Drs. Richard Kremer, Department of Medicine, McGill University, and Johng Rhim, NCI, National Institutes of Health, in the development of the HPK1A-*ras* cell line used in this work.

References

[1] Suda T, Shinki T, Takahashi N. The role of vitamin D in bone and intestinal cell differentiation. Annu Rev Nutr 1990;10:195–211.
[2] Jones G, Strugnell S, DeLuca HF. Current understanding of the molecular actions of vitamin D. Physiol Rev 1998;78:1193–231.
[3] Calverley MJ. Synthesis of MC903, a biologically active vitamin D metabolite analogue. Tetrahedron 1987;43:4609–20.
[4] Abe J, Morikawa M, Miyamoto K, Kaiho S, Fukushima M, Miyaura C, Abe E, Suda T, Nishii Y. Synthetic analogs of vitamin D_3 with an oxygen atom in the side chain skeleton: a trial of the development of vitamin D compounds which exhibit potent differentiation activation activity without inducing hypercalcemia. FEBS Lett 1987;226:58–62.
[5] Bretting C, Calverley MJ, Binderup L. Synthesis and biological activity of 1α-hydroxylated vitamin D_3 analogues with hydroxylated side chains, multi-homologated in the 24- or 24,26,27-positions. In: Norman AW, Bouillon R, Thomasset M, editors. Vitamin D_3 gene regulation, structure function analysis and clinical applications. Pro-

ceedings of the eighth workshop on vitamin D, Paris, France, 5–10 July 1991. Berlin: Walter de Gruyter, 1991.

[6] Dilworth FJ, Calverley MJ, Makin HLJ, Jones G. Increased biological activity of 20-epi-1,25-dihydroxyvitamin D_3 is due to reduced catabolism and altered protein binding. Biochem Pharmacol 1994;47:987–93.

[7] Siu-Caldera M-L, Sekimoto H, Peleg S, Nguyen C, Kissmeyer A-M, Binderup L, Weiskopf A, Vouros P, Uskokovic MR, Reddy GS. Enhanced biological activity of 1α,25-dihydroxy-20-epi-vitamin D_3, the C-20 epimer of 1α,25-dihydroxyvitamin D_3, is in part due to its metabolism into stable intermediary metabolites with significant biological activity. J Steroid Biochem Mol Biol 1999;71:111–21.

[8] Akiyoshi-Shibata M, Sakaki T, Ohyama Y, Noshiro M, Okuda K, Yabusaki Y. Further oxidation of hydroxycalcidiol by calcidiol 24-hydroxylase—A study with the mature enzyme expressed in *Escherichia coli*. Eur J Biochem 1994;224:335–43.

[9] Neef G, Kirsch G, Schwarz K, Wiesinger H, Menrad A, Fahnrich M, Thieroff-Ekerdt R, Steinmeyer A. 20-Methyl vitamin D analogues. In: Norman AW, Bouillon R, Thomasset M, editors. "Vitamin D. A pluripotent steroid hormone: structural studies, molecular endocrinology and clinical applications." Berlin: Walter de Gruyter, 1994. p. 97–8.

[10] Masuda S, Byford V, Kremer R, Makin HLJ, Kubodera N, Nishii Y, Okazaki A, Okano T, Kobayashi T, Jones G. *In vitro* metabolism of the vitamin D analog, 22-oxacalcitriol, using cultured osteosarcoma, hepatoma and keratinocyte cell lines. J Biol Chem 1996;271:8700–8.

[11] Reddy GS, Clark JW, Tserng K-Y, Uskokovic MR, McLane JA. Metabolism of 1,25-$(OH)_2$-16-ene D_3 in kidney: influence of structural modification of D-ring on side chain metabolism. Bioorg Med Lett 1993;3:1879–84.

[12] Masuda S, Strugnell S, Calverley M, Makin HLJ, Kremer R, Jones G. *In vitro* metabolism of the anti-psoriatic vitamin D analog, calcipotriol, in two cultured human keratinocyte models. J Biol Chem 1994; 269:4794–803.

[13] Strugnell S, Calverley MJ, Jones G. Metabolism of a cyclopropane-ring-containing analog of 1α-hydroxy-vitamin D_3 in a hepatocyte cell model. Identification of 24-oxidized metabolites. Biochem Pharmacol 1990;40:333–41.

[14] Makin G, Lohnes D, Byford V, Ray R, Jones G. Target cell metabolism of 1α,25-dihydroxyvitamin D_3 to calcitroic acid. Biochem J 1989;262:173–80.

[15] Henderson J, Sebag M, Rhim J, Goltzman D, Kremer R. Dysregulation of parathyroid hormone-like peptide expression and secretion in a keratinocyte model of tumor progression. Cancer Res 1991;51: 6521–8.

[16] Sebag M, Henderson J, Rhim J, Kremer R. Relative resistance to 1,25-dihydroxyvitamin D_3 in a keratinocyte model of tumor progression. J Biol Chem 1992;267:12162–7.

[17] Bligh EG, Dyer WJ. A rapid method of total lipid extraction and purification. Can J Biochem 1957;37:911–7.

[18] Jones G, Makin HLJ. Vitamin Ds: Metabolites and analogs. In: DeLeenheer AP, Lambert WE, Van Boxclaer JF, editors. "Modern chromatographic analysis of vitamins," 3rd ed., chap. 2. New York: Marcel Dekker, 2000. p. 75–142.

[19] Qaw F, Calverley MJ, Schroeder NJ, Trafford DJH, Makin HLJ, Jones G. *In vivo* metabolism of the vitamin D analog, dihydrotachysterol. J Biol Chem 1993;268:282–92.

[20] Makin HLJ, Jones G, Calverley MJ. Analysis of vitamin D, its metabolites and structural analogues. In: Makin HLJ, Gower DB, Kirk DN, editors. "Steroid analysis." Glasgow: Blackie, 1995. p. 562–620.

[21] Jones G, Byford V, Kremer R, Makin HLJ, Rice RH, deGraffenreid LA, Knutson JC, Bishop CA. Anti-proliferative activity and target cell catabolism of the vitamin D analog, 1α,24(S)-dihydroxyvitamin D_2 in normal and immortalized human epidermal cells. Biochem Pharmacol 1996;52:133–40.

[22] Shankar VN, Dilworth FJ, Makin HLJ, Schroeder NJ, Trafford DJH, Kissmeyer A-M, Calverley MJ, Binderup E, Jones G. Metabolism of the vitamin D analog EB1089 by cultured human cells: redirection of hydroxylation site to distal carbons of the side-chain. Biochem Pharmacol 1997;53:783–93.

[23] Dilworth FJ, Scott I, Green A, Strugnell S, Guo Y-D, Roberts EA, Kremer R, Calverley MJ, Makin HLJ, Jones G. Different mechanisms of hydroxylation site selection by liver and kidney cytochrome P-450 species (CYP27 and CYP24) involved in vitamin D metabolism. J Biol Chem 1995;270:16766–74.

[24] Yamada S, Yamamoto K, Masuno H, Ohta M. Conformation-function relationship of vitamin D: conformational analysis predicts potential side-chain structure. J Med Chem 1998;41:1467–75.

[25] Yamada S, Ino E, Takayama H, Horiuchi N, Shinki T, Suda T, Jones G, DeLuca HF. Differences in the side-chain metabolism of vitamin D_3 between chickens and rats. Proc Natl Acad Sci USA 1985;82: 7485–9.

[26] Danielsson C, Nayeri S, Wiesinger H, Thieroff-Ekerdt R, Carlberg C. Potent gene regulatory and antiproliferative activities of 20-methyl analogues of 1,25-dihydroxyvitamin D_3. J Cell Biochem 1996;63: 199–206.

[27] Jones G. Vitamin D and analogs. In: Bilezikian J, Raisz L, Rodan G, editors. Principles of bone biology, section III, chap. 77. San Diego: Academic Press, 1996. p. 1069–82.